DP-1311

TRANSPLUTONIUM CROSS SECTIONS DETERMINED IN A RESONANCE SPECTRUM IRRADIATION ASSEMBLY

J. D. SPENCER

K. W. MACMURDO

DU PONT

REG. U.S. PAT. OFF.

E. I. du Pont de Nemours & Co.
Savannah River Laboratory
Aiken, S. C. 29801

PREPARED FOR THE U. S. ATOMIC ENERGY COMMISSION UNDER CONTRACT AT(07-2)-1

Printed in the United States of America
Available from
National Technical Information Service
U. S. Department of Commerce
5285 Port Royal Road
Springfield, Virginia 22151
Price: Printed Copy $4.00; Microfiche $1.45

663349

DP-1311

UC-34c

TRANSPLUTONIUM CROSS SECTIONS DETERMINED IN A RESONANCE SPECTRUM IRRADIATION ASSEMBLY

by

J. D. Spencer

K. W. MacMurdo

Work done by

K. W. MacMurdo

J. D. Spencer

N. P. Baumann

M. C. Thompson

Approved by

R. L. Folger, Research Manager
Analytical Chemistry Division
and
P. L. Roggenkamp, Research Manager
Reactor Physics Division

Publication date: July 1974

E. I. du Pont de Nemours & Co.
Savannah River Laboratory
Aiken, S. C. 29801

PREPARED FOR THE U. S. ATOMIC ENERGY COMMISSION UNDER CONTRACT AT(07-2)-1

ABSTRACT

The design and use of a lithium-aluminum mockup of a resonance neutron spectrum irradiation assembly is described. Five of these neutron filter assemblies containing curium, californium, and reference foils of ^{235}U and ^{239}Pu were irradiated in a Savannah River Plant reactor. The irradiation spectrum was similar to that of a reactor in which a large fraction of the D_2O moderator space is displaced with magnesium. Four of these capsules contained lithium-aluminum alloy, and one contained only aluminum to retain the nominal reactor spectrum. Irradiation products were chemically separated, and their concentrations determined by chemical recovery and analytical techniques developed during this study.

Burnup and production were calculated for each sample. Comparison of calculations with measurements indicated that the initial ^{244}Cm cross section was too high and the cross sections for ^{250}Cf, ^{251}Cf and ^{252}Cf needed some adjustment. Recommendations for changes to these cross sections cannot be made because the method of creating a total effective cross section for the production calculations probably contains errors. Additional computations with effective cross sections derived from multigroup flux, and cross section representation for samples irradiated in a variety of neutron spectra should permit more nearly quantitative recommendations for improvements in cross section data.

CONTENTS

LIST OF FIGURES

LIST OF TABLES

TRANSPLUTONIUM CROSS SECTIONS DETERMINED IN A RESONANCE SPECTRUM IRRADIATION ASSEMBLY

INTRODUCTION

Improving production of ^{252}Cf at the Savannah River Plant (SRP) was initially directed toward achieving as high a thermal flux[1] (high flux concept) as feasible in one of the reactors. With this concept, production is enhanced greatly because the time for each of the many successive neutron captures is very much shortened. Two high flux campaigns have made more than 3 g of ^{252}Cf.

An alternative approach toward improved ^{252}Cf production was suggested by theoretical predictions[2] of the capture-to-fission cross section ratios of the nuclides in the production chain. These predictions indicated significant gains might be realized by irradiating the feed material in a neutron energy spectrum with a higher epithermal-to-thermal flux ratio than that of the high flux or normal loadings. This approach resulted in the concept of the Magnesium Displaced-Moderator Resonance Reactor.[3] In this concept, most of the heavy water moderator was replaced with cylindrical magnesium logs. With the moderator removal, a neutron energy spectrum was obtained in which most of the neutron capture reactions occurred above thermal energies, in the resonance region.

During evaluation of the resonance reactor concept, a companion program was started to upgrade cross section data for the nuclides in the ^{252}Cf production chain. When this program was begun, only limited differential cross section data were available for the curium and californium isotopes (Figure 1), and there were large uncertainties in the integral cross sections of many of the isotopes. In addition, total effective cross sections formulated from these integral values could lead to large errors in production estimates in reactor irradiations where significant reactions occur above thermal energies.

The study described in this report was designed to assist in the evaluation of the accuracy of the curium and californium cross sections, and to develop an appropriate method to measure effective cross sections for nonthermal reactor spectra.

Computations indicated that the well-thermalized neutron spectrum in SRP reactors could be converted to a resonance spectrum in a foil irradiation assembly by surrounding the assembly with a thermal neutron absorbing material.

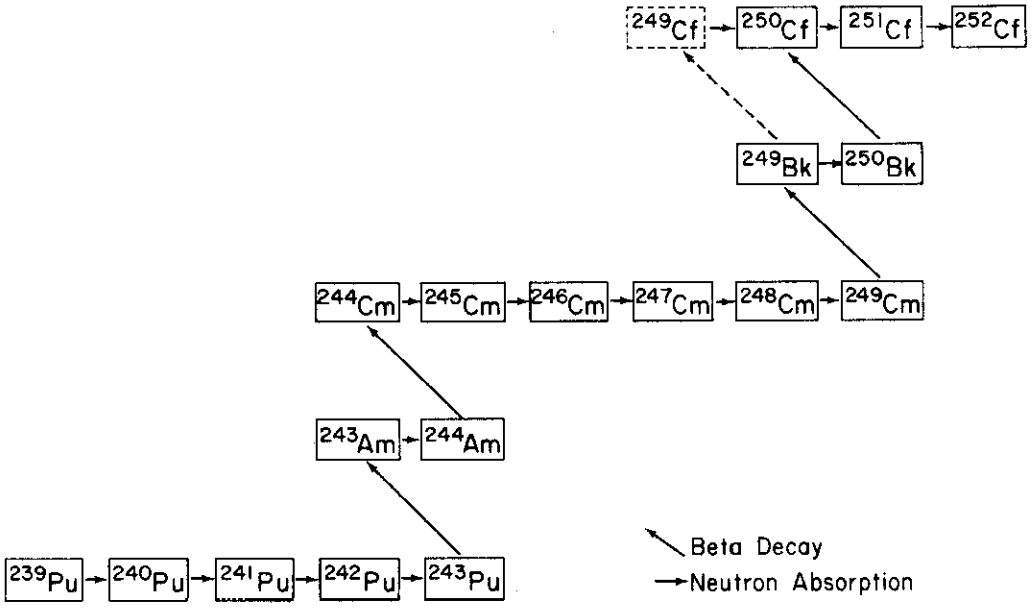

FIGURE 1. CALIFORNIUM-252 PRODUCTION CHAIN

Since only limited quantities of the desired target material were available, irradiations would have to be performed in the production reactors to get measurable changes in isotopic content. Foils were prepared and an assembly designed[4] to modify the neutron spectrum, i.e., to act as a neutron filter. If a material having a 1/v absorption cross section was used for this filter, then the Maxwellian peak in the well-thermalized distribution could be diminished. The irradiation spectrum would then be similar to that of the Magnesium Displaced Moderator Resonance Reactor. A calculated neutron energy spectrum for the resonance reactor is shown in Figure 2 along with a typical thermal reactor spectrum. For a 1/v absorber in a thermal spectrum, most of the reactions occur with neutrons whose energies are primarily in the vicinity of the large Maxwellian peak; but in the resonance spectrum, the majority of the reactions occur near the cadmium cutoff ($\sim$0.5 eV).

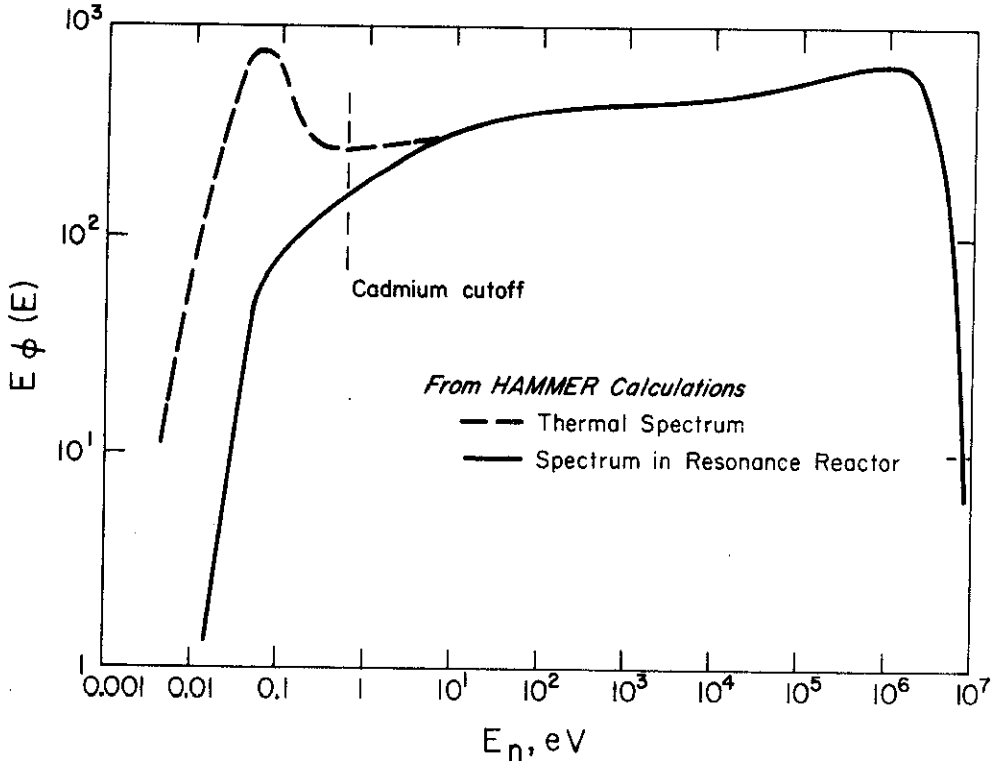

FIGURE 2. NEUTRON SPECTRA

SPECTRUM WITHIN THE NEUTRON FILTER ASSEMBLY

Initial scoping studies were made with the assembly shown in Figure 3. Powdered alumina and amorphous boron were mixed in several different ratios to achieve a variation in neutron absorption and, hence, in the hardness of the spectrum. The spectrum was characterized for each mixture by measuring the cadmium ratios of ^{235}U, ^{239}Pu, and ^{63}Cu foils. The test irradiations were made with the filter assembly positioned in the axial center of a fuel assembly consisting of three thin, concentric ^{235}U-Al tubes with average diameters of 2.32, 2.48, and 3.62 inches. Calculated spectra are shown in Figure 4, including that for the resonance reactor. The reduction in the Maxwellian peak is apparent as the boron concentration is increased. These results were used to specify a 0.79 wt % ^{6}Li concentration in the lithium-aluminum alloy assembly designed (Figure 5) for final irradiation. The ^{6}Li-Al alloy was chosen because of its ready availability and well-characterized irradiation behavior.

The spectrum was measured with an irradiation assembly containing 0.79 wt % ^{6}Li material to verify the HAMMER[5] calculated spectrum. This spectrum was measured in a zero-power, heavy-water-moderated reactor lattice similar to the lattice of a production reactor. The detector foils used to characterize this spectrum are listed in Table I. Conventional techniques were used to analyze the epicadmium resonance detectors ^{115}In, ^{197}Au, ^{186}W, and ^{63}Cu. The analyses of the foil data and the derivation of the flux at the resonance energies are discussed in Appendix A. For all foils, the activation rates in the filter assembly were compared with those obtained simultaneously in a well-thermalized flux. Based on the thermal cross section and the resonance integral of each isotope, the flux at the resonance energy was evaluated.

The analyses of the ^{176}Lu and ^{239}Pu subcadmium resonances required a different technique. For these isotopes, a resonance integral was derived by numerically integrating the subcadmium differential cross sections. The measured activities of these isotopes were also corrected for reactions that occurred in the regions above and below the resonance. The details are discussed in Appendix A.

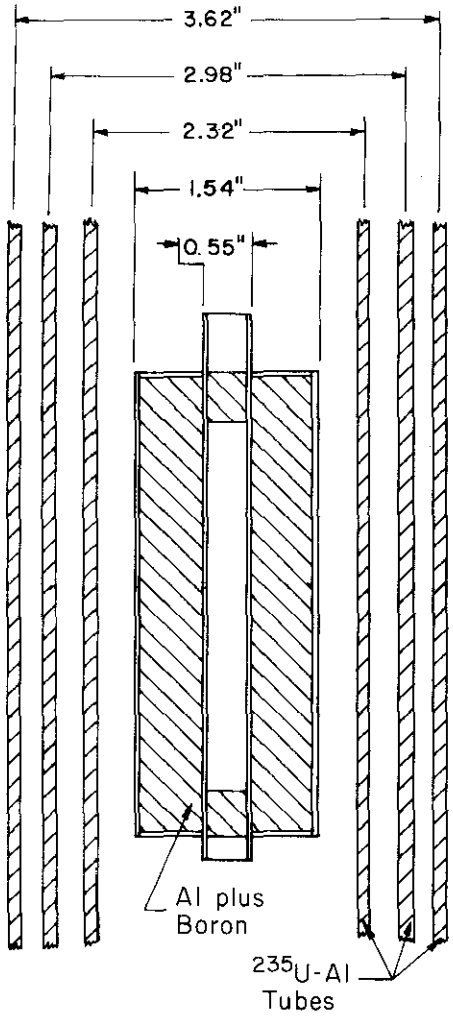

FIGURE 3. ALUMINUM - BORON TEST ASSEMBLY

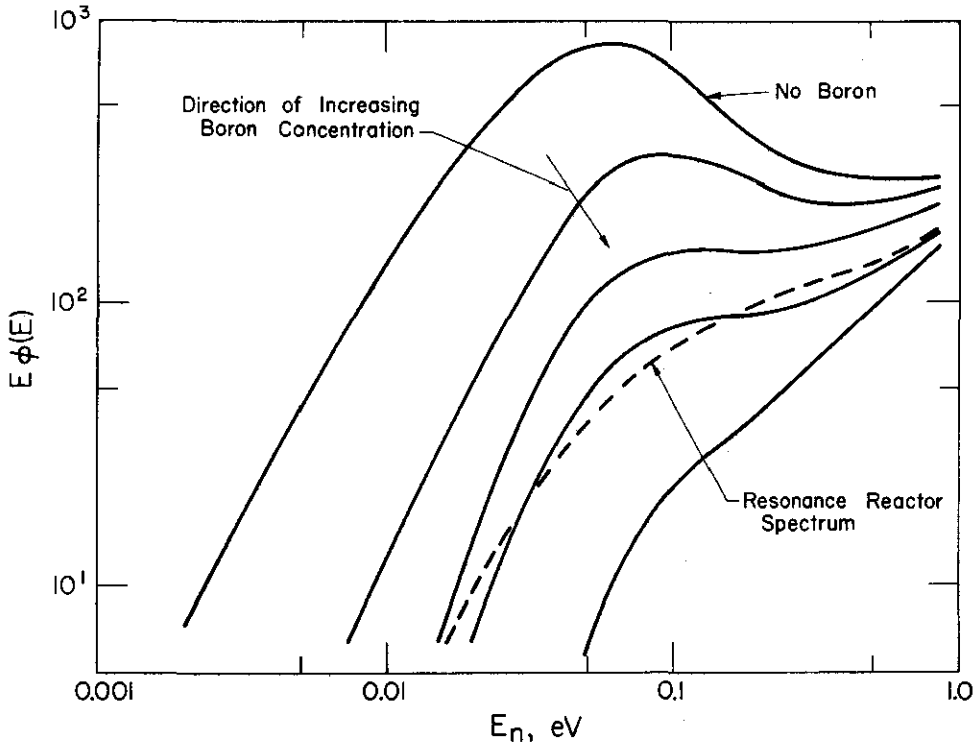

FIGURE 4. NEUTRON SPECTRA FOR VARIOUS BORON CONCENTRATIONS

TABLE I. Resonance Detectors

Isotope	Resonance Energy, eV
^{176}Lu	0.143
^{239}Pu	0.296
^{115}In	1.46
^{197}Au	4.91
^{186}W	18.8
^{63}Cu	580.

FOIL IRRADIATION

Four Li-Al alloy filter assemblies and one identical assembly containing no Li-Al alloy were prepared for irradiation in an SRP reactor. Each assembly contained duplicate aluminum foil specimens enriched in ^{235}U, ^{239}Pu, and ^{244}Cm. These nuclides were deposited on high-purity aluminum foils, which in turn were rolled into cylinders and sealed in quartz ampoules (Figure 5).

The isotopic contents of the ^{244}Cm and ^{239}Pu samples were derived from a combination of gross alpha counting, alpha pulse height analysis, and mass spectrometry. Before irradiation, more than 99.9% of the californium isotopes was removed from the curium samples.

The ^{235}U samples were assayed by coulometry and mass spectrometery because the ^{235}U alpha activity was too low to measure directly. Isotopic analyses and contents of these curium foils before and after irradiation are shown in Tables II and III.

The five assemblies were irradiated from one to four months with no operational difficulties. Activation rates were measured in these assemblies with reference foils of ^{235}U and ^{239}Pu and for various curium and californium isotopes in the ^{252}Cf production chain. The predominant isotopes; the irradiation time; the burnup of ^{244}Cm, ^{235}U, and ^{239}Pu; and the cycle-average fast-to-slow neutron flux ratios are included in Table IV for each of the filter assemblies.

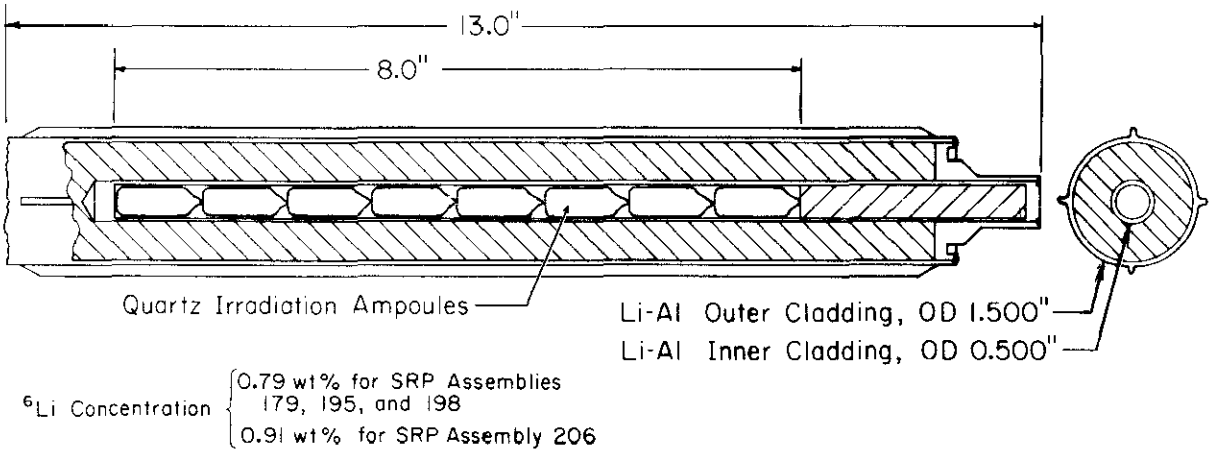

FIGURE 5. LITHIUM - ALUMINUM ALLOY ASSEMBLY

TABLE II. Measured and Calculated Concentrations for Assembly No. 207 (Bare Al)

	Measured		Calculated		
			Current Set[a]		After 27% Reduction of ^{244}Cm I_{Abs}^{∞}
Isotopes	Initial	Final	Normalized to ^{235}U Fissions[b]	Normalized to ^{244}Cm Atom Fraction[c]	Normalized to ^{244}Cm Atom Fraction[c]
^{243}Cm	0.000268	-	-	-	
^{244}Cm	1.000	0.8948	0.837	0.923	0.890
^{245}Cm	0.00831	0.0308	0.0444	0.0386	0.0308
^{246}Cm	0.04397	0.05281	0.0578	0.0485	0.0526
^{247}Cm	0.000737	0.001357	0.00157	0.00110	0.00144
^{248}Cm	0.0004217	0.0005647	0.000586	0.000478	0.000546
^{250}Cf	-	3.04×10^{-6}	5.67×10^{-6}		4.8×10^{-6}
^{252}Cf	-	2.31×10^{-6}	1.46×10^{-6}		1.0×10^{-6}
Total Fissions	-	0.051 ±0.005			

Reference Foils

	Initial Conc.	Total Fissions
^{235}U	1.000	0.449

a. Cross sections in Appendix B.
b. Calculated concentration at time where measured and calculated number of ^{235}U fissions agree.
c. Calculated concentration at time where measured and calculated ^{244}Cm atom fraction agree.

TABLE III. Measured and Calculated Concentrations for Assembly No. 206 (^{6}Li-Al Alloy)

	Measured		Calculated		
			Current Set[a]		After 27% Reduction of ^{244}Cm I_{Abs}^{∞}
Isotopes	Initial	Final	Normalized to ^{235}U Fissions[b]	Normalized to ^{244}Cm Atom Fraction[c]	Normalized to ^{244}Cm Atom Fraction[c]
^{243}Cm	0.000268	-			
^{244}Cm	1.000	0.9215	0.896	0.930	0.921
^{245}Cm	0.00831	0.05537	0.0757	0.057	0.0550
^{246}Cm	0.04397	0.04485	0.0458	0.0446	0.0451
^{247}Cm	0.000737	0.00121	0.00137	0.00117	0.00138
^{248}Cm	0.0004217	0.00046	0.00048	0.000457	0.000486
^{250}Cf	-	1.87×10^{-6}	1.81×10^{-6}		1.87×10^{-6}
^{252}Cf	-	1.91×10^{-7}	0.408×10^{-7}		0.438×10^{-7}
Total Fissions		0.011 ±0.001			

Reference Foils

	Initial Conc.	Total Fissions
^{235}U	1.000	0.085

a. Cross sections in Appendix B.
b. Calculated concentration at time where measured and calculated number of ^{235}U fissions agree.
c. Calculated concentration at time where measured and calculated ^{244}Cm atom fraction agree.

TABLE IV. Resonance Mockup Irradiations

Sample	Isotopes	^{244}Cm Burnup, %	^{235}U Fissioned, %	^{239}Pu Fissioned, %	(ϕ_f/ϕ_s) Cycle Avg.
179 (Li-Al)	^{244}Cm, ^{249}Cf	3.0	2.3		12.2
195 (Li-Al)	^{244}Cm, ^{245}Cm, ^{246}Cm	3.7	3.5	7.8	12.1
198 (Li-Al)	^{244}Cm, ^{246}Cm, ^{249}Cf	7.8	7.9	23.6	11.7
206 (Li-Al)	^{244}Cm	7.9	8.5	--	11.2, 9.75[a]
207 (Bare Al)	^{244}Cm	10.1	44.9	--	2.19

a. Separated into two cycles with these average fast-to-slow flux ratios for the calculations (see Figure 8).

ANALYSIS OF IRRADIATED FOILS

Specimen Preparation

The assemblies were allowed to cool for approximately five months before the quartz ampoules were removed. To prevent contamination from the outside of the quartz, the unopened ampoules were leached in dilute nitric acid. Each ampoule was then crushed, and the aluminum foil containing the active material was removed. Care was taken to ensure that no cross contamination occurred during the process of opening the ampoules.

Similar chemical preparations and analysis techniques were used for all of the foils included in the various irradiations; however, analysis of foils from the final two assemblies (No. 206 and 207) included certain refinements which improved the overall quality of the data. The discussion of the analytical techniques will be limited to those used to analyze these foils, although data from all of the assemblies are included in a later section of this report.

Each sample was dissolved separately in a solution of 8M HNO_3 containing a drop of mercuric nitrate catalyst. After dissolution, each sample was quantitatively transferred to a volumetric flask and diluted to 10.00 ml. Aliquots were taken from each ten ml dilution, and further diluted to 5.00 ml for absolute gamma counting. The sizes of the aliquots were chosen so that the dead times registered on the 4096-channel pulse height analyzer (PHA) were approximately 20%.

Determination of Total Fissions

The numbers of fissions in each sample was determined by measuring the gamma activity from the fission product ^{137}Cs. This isotope has a high fission yield, and the decay scheme is well characterized. The ^{137}Cs fission yield is well known for ^{235}U and ^{239}Pu[6] fission and was recently measured for ^{245}Cm,[7] the isotope which undergoes the majority of the fissions during the irradiation of the ^{244}Cm sample. The ^{137}Cs gamma activity of each sample was measured with a 45 cm^3 Canberra Ge(Li) detector* with a resolution of 2.6 keV at full width-half maximum (FWHM) at 1332.5 keV. The ^{137}Cs photopeak areas were determined by subtracting the Compton background from the total counts. A ^{137}Cs standard was counted in the same geometric configuration to determine counting efficiency. Corrections

---

* Product of Canberra Industries, Inc., Meriden, Conn.

were made for the overall counting efficiency, the branching ratio, the sample dilution factor, and the decay since the end of the irradiation. These corrections were necessary to evaluate the absolute number of fissions; however, the ratios of fissions in the curium, ^{235}U, or ^{239}Pu samples could be found directly from the uncorrected data.

Determination of Curium Isotopic Content

Alpha counting and mass spectrometric analyses were used to characterize the concentrations of the various curium isotopes following the irradiation. Gross alpha analyses gave the total curium activities of the original dilutions, and alpha pulse height analyses and mass spectrometry gave the curium isotopic compositions.

Further dilutions were made from the dissolved curium solution in 0.1M HNO_3, and aliquots of each sample were mounted on stainless steel counting plates for the gross alpha determinations. The counting rates were measured in a gas-flow proportional counter.

The high aluminum nitrate content in the curium samples had to be eliminated before mass spectrometric analyses and before suitable electrodeposited mounts of the irradiated curium could be prepared for the alpha pulse height analyses. Dissolved aluminum was separated from the curium samples by coprecipitating the curium with ferric hydroxide. The hydroxide was dissolved in 8M HCl, and the iron was removed by a *Dowex** 1-X8 anion exchange column in the chloride form. Conversion of the sample from the chloride to the nitrate form completed the cleanup procedure. Electrodeposited mounts of the curium samples were prepared on one-inch-diameter platinum discs by a standard electrodeposition procedure from a 6M NH_4Cl electrolyte.

Alpha pulse height measurements to determine curium purity were made with a room temperature surface barrier detector in a vacuum system coupled to standard low noise electronics and a 400-channel pulse height analyzer. Typical resolution for the 5.801 MeV ^{244}Cm alpha transition was 15 to 17 keV (FWHM). Results of the alpha pulse height analyses showed no detectable alpha activities other than ^{244}Cm.

---

* Registered trademark of Dow Chemical Co., Midland, Mich.

Mass spectrometry was used to determine the isotopic fraction of each curium isotope. The mass spectrometric analyses of the irradiated curium samples were determined in a 13.5 inch radius Avco single-focusing mass spectrometer* with a triple filament ion source. Sample sizes of 20 to 30 nanograms of curium were required for mass analyses. Duplicate samples were obtained from the contents of each ampoule, and multiple mass analyses were obtained for each sample in assemblies No. 206 and 207. These results were used to estimate the uncertainties in the isotopic content for each foil. The mass spectrometric data for each sample are listed in Tables II and III.

Californium - Curium Separation Procedure

A cation exchange procedure was developed that was capable of quantitatively separating and purifying the part per million-level californium produced during the irradiation from the bulk of the curium. Determination of the amount of ^{250}Cf and ^{252}Cf produced in the irradiation was accomplished by alpha pulse height analysis after the conversion of the separated californium-isobutyrate solution to the nitrate form and quantitative electrodeposition. ^{251}Cf was not detectable by either alpha counting or mass spectrometric analysis.

The cation exchange column was a 4-mm-diameter, thick-walled capillary tube. Platinum tubing 1/2 inch in length and 0.0145 inch in diameter was sealed into the end of the column so that uniform droplets of 18λ volume could be collected. The capillary tube was partially filled with 450λ of extensively graded *Dowex* 50W-X8 cation exchange resin of 18±1 μm diameter particle size. Experiments have shown that the use of graded resin greatly increases the sharpness of separation.[8] The column was maintained at 80°C during the separation. Pressure was maintained above the resin bed to give a flow rate of 2 drops per minute. The samples were eluted with ammonium alpha-hydroxyisobutyrate (AHIB) of pH 4.60. A known amount of ^{160}Tb tracer was added during each column separation. Terbium elutes just ahead of californium in the isobutyrate system and served as a monitor on the location of the californium elution peak and also allowed the sharpness of the elution profile to be checked for each process run. Drops were collected in small glass vials at the bottom of the column. ^{160}Tb gamma activity in the collection vials was detected by a 2-inch x 2-inch NaI detector and a single channel analyzer bracketing the unresolved 879, 962 and 966-keV gamma transitions. An in-line alpha probe with a rate meter was used to detect the californium alpha activity as it emerged

---

* Product of Avco Corp., Cincinnati, Ohio

from the column and to check for breakthrough of the curium. The column was loaded by equilibrating the samples with 20λ of graded *Dowex* 50W-X8 resin in 0.05M HNO_3. Checks for ^{160}Tb and gross alpha activity in the supernates showed that more than 99% of the activity was adsorbed consistently. The equilibrated resin was transferred to the top of the cation exchange column, and a column volume of water was passed through the column to remove the nitric acid before eluting with isobutyrate. Six drops per vial were collected until ^{160}Tb was detected at which time collection was reduced to 3 drops per vial.

Several trial runs with known quantities of terbium, californium, and curium were made to standardize the cation exchange column, i.e., to determine the elution peak positions and profiles of each species, the decontamination factors, and and the percent recovery of terbium and californium. In all cases, elution was stopped after the californium was eluted. The trial runs showed that recovery yields of both terbium and californium were essentially 100%, and the decontamination factor from curium was about 10^5.

Determination of Californium Following Irradiation

After separation, the vials containing californium were combined, sampled for a gross alpha count, and adjusted to 0.25M in HNO_3. The sample was then loaded on a second *Dowex* 50W-X8 graded cation exchange column preconditioned with 0.25M HNO_3. Ten column volumes of 0.25M HNO_3 were washed through the column to remove the alpha-hydroxyisobutyrate. The californium was then quantitatively stripped off the column with 5M HNO_3. The sample was reduced to dryness with concentrated nitric acid several times under a heat lamp and diluted to 1.00 ml with 0.05M HNO_3. A 10λ gross alpha mount was prepared and counted to determine the percent recovery of californium. The entire sample was then electrodeposited from 6M NH_4Cl onto a one-inch-diameter platinum plate. A gross alpha count of the electrodeposited mount gave the percent californium electrodeposited. Alpha pulse height analyses gave the relative amounts of ^{250}Cf and ^{252}Cf present. The recovery data for the separation and conversion columns and for the electrodeposition allowed calculation of the total ^{250}Cf and ^{252}Cf in the irradiated curium samples. Duplicate separations and analyses on each sample provided a useful check on the accuracy of the entire process of separation and analysis. Insufficient quantities of ^{250}Cf and ^{252}Cf were produced in the irradiation for a mass spectrometric analysis.

MASS BALANCE CONSIDERATIONS

Absolute gamma counting and the previously measured ^{137}Cs fission yield of 6.14%[7] from the thermal-neutron induced fission of ^{245}Cm allowed the total fissions in each curium sample to be calculated. This fission information was necessary to determine the mass balance for each sample where the total number of curium atoms before irradiation should equal the number of atoms of curium, berkelium, and californium recovered, plus the number of fissions. Fortunately the amount of berkelium and californium produced as capture products was insignificant in mass balance considerations and is not discussed further. The mass balance corrections are included in the measured final concentrations listed in Tables II and III. The initial mass concentrations were measured before irradiation and are not decay corrected to the end of irradiation. Corrected for decay, the initial and final mass volumes agree to within 0.1%. The total fissions measured in the curium and uranium foils also are shown in Tables II and III.

CALCULATION OF THE NEUTRON SPECTRUM DURING IRRADIATION

The theoretical evaluation of the isotopic content of the samples following irradiation requires knowing the neutron flux at the sample, the effective cross section of each isotope, and the time history of the irradiation. The magnitude of the flux and the effective cross sections are constantly changing during the irradiation from the ^{235}U burnup in the fuel and the ^{6}Li burnup in the filter assembly. The extent of these changes was evaluated for the various irradiation cycles with the HAMBUR[9] code.

Spectral measurements with the filter assembly (see Appendix A) indicated that HAMBUR predicted a harder spectrum than actually existed. The ^{6}Li concentration was reduced in the computational model until the calculated spectral index (^{235}U cadmium ratio) agreed with the measured result. This "normalized" ^{6}Li loading was then used in HAMBUR as the initial concentration. Figure 6 shows the reactor relative power history from operating data for assemblies No. 206 and 207 and average values (derived from integrated power over indicated time span) of this relative power for the two main cycles.

The foil data were corrected for thermal and resonance self-shielding, nonresonance activation, and resonance overlap by cadmium and ^{235}U in the fuel. Figure 7 illustrates the measured and calculated spectrum for the ^{6}Li-Al filter assembly (No. 206). The measured data were normalized so that the flux at the gold

resonance coincides with the calculated distribution. These data indicate that the shape of the derived spectrum matches the calculated distribution reasonably well. The slightly higher distribution measured in the subcadmium region was also evident

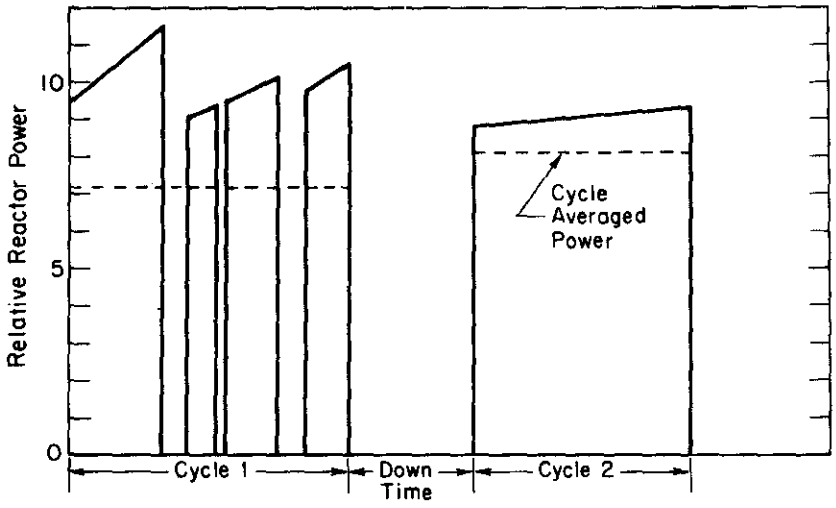

FIGURE 6. RELATIVE REACTOR POWER HISTORY FOR SLUGS NOS. 206 AND 207

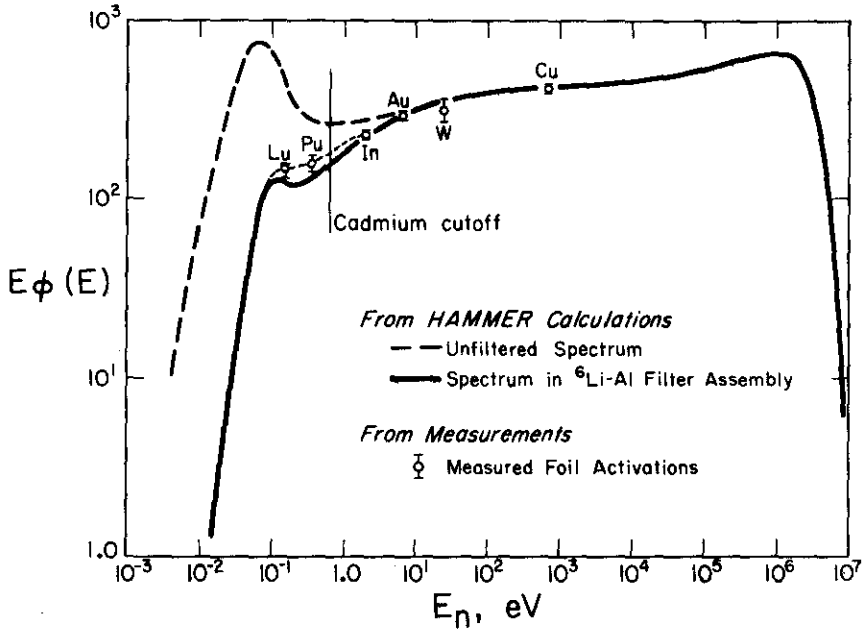

FIGURE 7. Li-Al ALLOY FILTER SPECTRA

in the measured ^{235}U cadmium ratio, which was larger than the calculated value.

HAMBUR predictions of changes in the fast-to-slow flux ratio and the relative value of the thermal flux are shown in Figures 8 and 9 for the bare (No. 207) and the ^{6}Li-Al (No. 206) assemblies. Because the variation between the ϕ_f/ϕ_s ratio and ϕ_s was small for the bare assembly over the irradiation cycle, average values were used in the production calculations. The variation in the spectrum in the ^{6}Li-Al alloy assembly was greater. Therefore, different average values were used in each of the two main subcycles. The computer code for calculating isotopic composition contains coupled differential equations that treat the time behavior of isotopic mixtures during and after irradiation.

The effective cross sections used in the production calculations and the spectral indexes for assemblies No. 206 and No. 207 are listed in Table V. These effective cross sections were derived from the data presented in Appendix B for the given (ϕ_f/ϕ_s). The effective cross sections for assemblies 179, 195, and 198 were

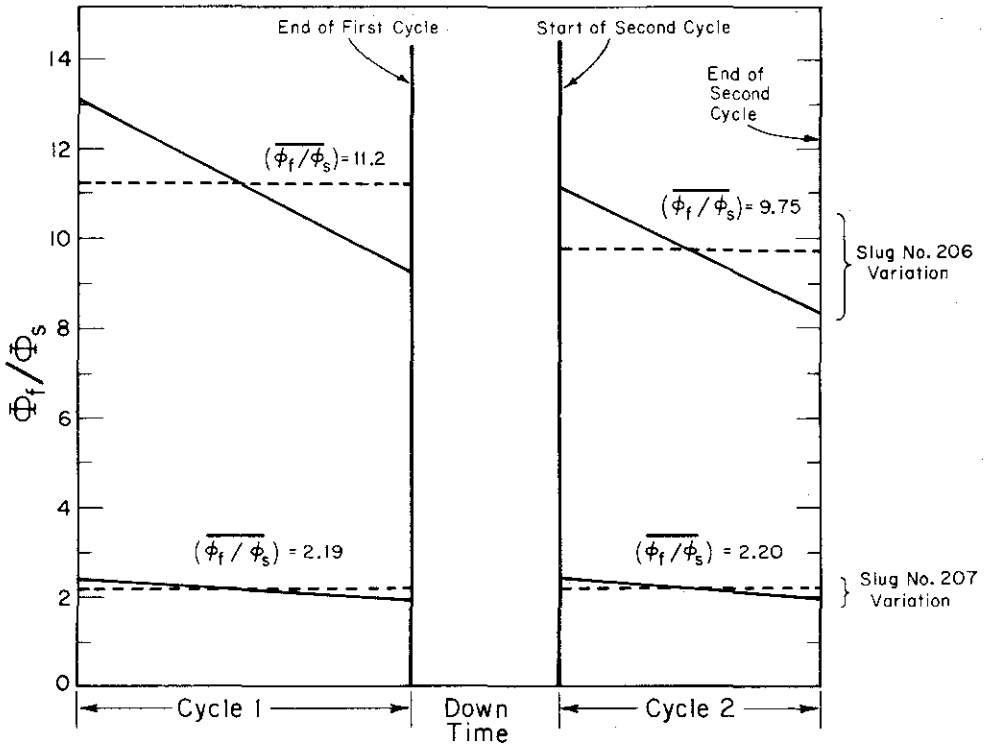

FIGURE 8. FAST-TO-SLOW FLUX RATIO HISTORY FOR SLUGS NOS. 206 AND 207

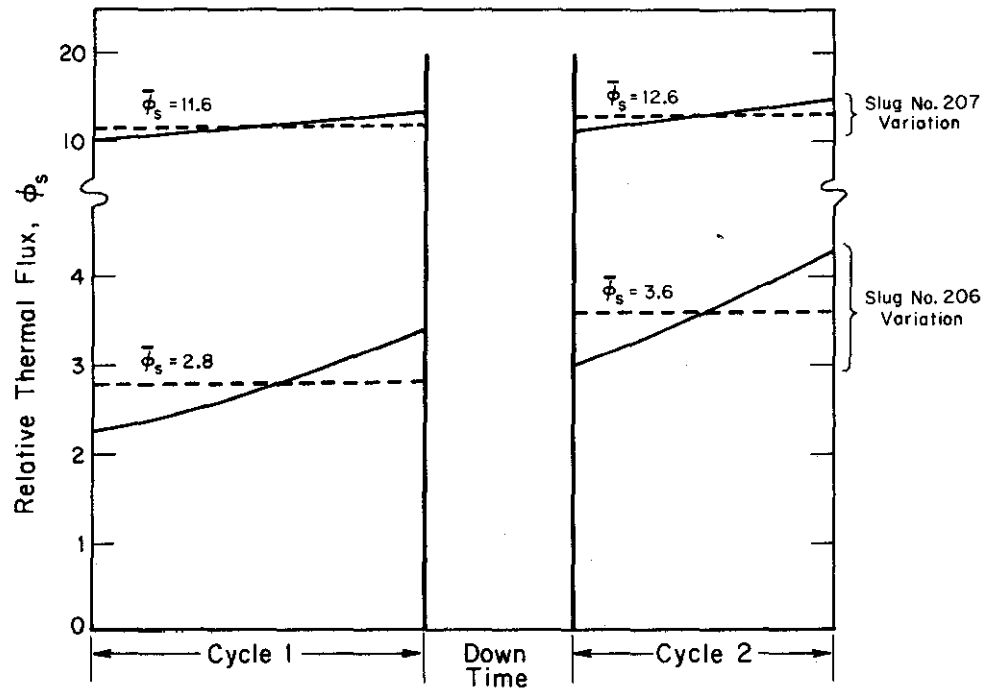

FIGURE 9. RELATIVE THERMAL FLUX HISTORY FOR SLUGS NOS. 206 AND 207

TABLE V. Effective Cross Sections for Assemblies No. 206 and No. 207

	No. 207 (Bare Al)			No. 206 (^{6}Li-Al Alloy)					
	(ϕ_f/ϕ_s) = 2.19			1st Cycle (ϕ_f/ϕ_s) = 11.2			2nd Cycle (ϕ_f/ϕ_s) = 9.75		
Isotope	$\overline{(\sigma_A^{th})}$	$\overline{(\sigma_A^{epi})}$	$\overline{(\sigma_A^{tot})}$	$\overline{(\sigma_A^{th})}$	$\overline{(\sigma_A^{epi})}$	$\overline{(\sigma_A^{tot})}$	$\overline{(\sigma_A^{th})}$	$\overline{(\sigma_A^{epi})}$	$\overline{(\sigma_A^{tot})}$
^{244}Cm	9.45[a]	75[a]	84.4	5.97[a]	320	326	6.24[a]	283[a]	289
^{245}Cm	1708	103	1811	952.5	436	1398	1005	384	1389
^{246}Cm	0.848	13.8	14.6	0.567	66.0	66.6	0.588	57.7	58.3
^{247}Cm[b]	106	144	250	67	610	677	70	538	608
^{248}Cm	0.93	27.5	28.4	0.59	123	123	0.62	110	111
^{249}Bk	1001	137	1138	638	580	1218	666	513	1179
^{249}Cf	1311	302	1613	836	1230	2066	872	1105	1977
^{250}Cf	1025	540	1565	653	2120	2773	682	1950	2632
^{251}Cf	4768	232	5000	3040	940	3980	3172	838	4010
^{252}Cf	19.3	6.8	26.1	12.3	33.0	45.3	12.9	28.7	41.6
1/V	0.690	0.042	0.732	0.440	0.182	0.622	0.459	0.161	0.620

a. The values of the effective cross sections were obtained from Figures B-1 and B-3 for the spectral index (ϕ_f/ϕ_s) listed above. The derivation of these data is discussed in Appendix B. The base cross section set is from Table B-1 in Appendix B.

b. For isotopes ^{247}Cm → ^{252}Cf, the $\overline{(\sigma_A^{th})} = \left(\frac{\sigma_A}{\sigma_{2200}}\right)_{1/V} \times (\sigma_{2200})_i$

obtained in an identical fashion for the cycle-averaged flux-ratios listed in Table IV.

CALCULATION OF THE ISOTOPIC CONTENT FOLLOWING IRRADIATION

The effective cross sections and fluxes (Figures 8, 9, and Table V) were input to a computer code along with the initial isotopic concentrations of the ^{235}U, ^{239}Pu, and the curium foils. The code then calculated the concentration for each isotope as a function of time. If the absolute thermal flux was known accurately, the output could be examined at a ($\phi_s t$) corresponding to the particular cycle, and a direct comparison with the measured results would be possible. In most cases, ϕ_s was not known well enough for this procedure to be successful.

An alternate approach compared the calculated number of ^{235}U fissions to the measured fissions in the reference foil. This approach generally improved the agreement between measurements and calculations. However, some cases still exhibited a particularly poor comparison, which was possibly caused by difficulties in absolute fission product counting in the ^{235}U reference foils.

An approach not requiring ($\phi_s t$) or reference foil normalization was also examined. The calculations were normalized at the experimentally measured atom fraction of ^{244}Cm. The calculated concentrations of each of the curium isotopes was then compared to the measured results. In most cases, this approach yielded the best agreement between measurements and calculations, particularly after the reduction in the ^{244}Cm effective cross section was made.

COMPARISON OF MEASURED AND CALCULATED ISOTOPIC CONCENTRATIONS

The measured and calculated concentrations and atom fractions for the various samples are presented in Tables II, III, VI, VII and VIII. The assemblies with the largest burnups (No. 206 and 207) are discussed first, as the validity of the formulation in the computer code of the effective cross section can be evaluated more accurately with these samples.

TABLE VI. Measured and Calculated Concentrations for Assembly No. 198 (Li-Al)

Isotope	Concentration			Atom Fraction			
	Initial, Meas.	Final, Meas.	Final, Calc.	Initial, Meas.	Final, Meas.	Final, Calc.	Final, Calc. 27% Red. ^{244}Cm I^{∞}_{Abs}
198-1; 195-3: 57.79 a/o ^{244}Cm							
^{244}Cm	1.000	0.9195		0.5779	0.5556	0.555[a]	0.556[a]
^{245}Cm	0.007944	0.03368		0.00459	0.0203	0.0311	0.0311
^{246}Cm	0.3593	0.3547		0.2075	0.2146	0.211	0.213
^{247}Cm	0.3424	0.3060		0.1977	0.1849	0.182	0.174
^{248}Cm	0.02127	0.04157		0.0123	0.0246	0.0209	0.0255
Fissions	-	0.07637					
198-2; 195-2: 94.66 a/o ^{246}Cm							
^{244}Cm	0.05343	0.04944		0.0506	0.0475	0.0476	0.0483
^{245}Cm	0.001701	0.002592		0.00161	0.00249	0.00339	0.00276
^{246}Cm	1.000	0.9811		0.9466	0.9397	0.9397[b]	0.9397[b]
^{247}Cm	0.0006778	0.007077		0.00064	0.00678	0.00883	0.00897
^{248}Cm	0.0006579	0.003688		0.0062	0.00354	0.0008	0.0008
Fissions	-	0.01252		-			
198-3: 100 a/o ^{249}Cf							
^{249}Cf	1.000	0.625	.625[c]	1.000	0.8695		
^{250}Cf	-	0.0580	.061	-	0.0807		
^{251}Cf	-	0.0268	.0198	-	0.0373		
^{252}Cf	-	0.0089	.0070	-	0.0124		
^{253}Cf	-	1.36×10^{-5}	0.99×10^{-5}	-	0.00002		
Fissions	-	0.281					
198-4: 39.75 a/o ^{249}Cf							
^{249}Cf	1.000	0.6257	0.625[c]	0.3975	0.3109		
^{250}Cf	0.5580	0.3014	0.297	0.2218	0.1498		
^{251}Cf	0.1784	0.1832	0.214	0.0709	0.0910		
^{252}Cf	0.7789	0.8997	0.909	0.3097	0.4470		
^{253}Cf	-	0.002648	0.00243	-	0.0013		
Fissions		0.5024					

Reference Foils

Isotope	Initial Conc.	Total Fissions
^{239}Pu	1.000	0.236 ±0.014
^{240}Pu	0.0518	
^{241}Pu	0.0010	
^{235}U	1.000	0.0788 ±0.006

a. Atom fractions evaluated at exposure where measured and calculated ^{244}Cm atom fraction agree.
b. Atom fractions evaluated at exposure where measured and calculated ^{246}Cm atom fraction agree.
c. Atom fractions evaluated at exposure where measured and calculated ^{249}Cf atom fraction agree.

TABLE VII. Measured Isotopic Concentrations for Assembly No. 195 (Li-Al)

195-1: 76.8 a/o ^{245}Cm

Isotope	Initial	Final
^{244}Cm	0.2976	0.2831
^{245}Cm	1.000	0.9067
^{246}Cm	0.004365	0.0156
Total Fissions	-	0.09656

195-2: 94.68 a/o ^{246}Cm

^{244}Cm	0.05308	0.05124
^{245}Cm	0.001701	0.002398
^{246}Cm	1.000	0.9965
^{247}Cm	0.0006764	0.003402
^{248}Cm	0.0006559	0.001742
Fissions	-	0.0007378

195-3: 57.79 a/o ^{244}Cm

^{244}Cm	1.000	0.9723
^{245}Cm	0.007944	0.02107
^{246}Cm	0.3593	0.3634
^{247}Cm	0.3424	0.3321
^{248}Cm	0.02127	0.02327
Fissions	-	0.01845

Reference Foils

Isotope	Initial Conc., Meas.	Total Fissions
^{239}Pu	1.000	
^{240}Pu	0.0518	0.078
^{241}Pu	0.0010	
^{235}U	1.000	0.03485

Cobalt (at discharge) = 7.97×10^{12} disintegrations/minute-gram

TABLE VIII. Measured and Calculated Concentrations for Assembly No. 179 (Li-Al)

179-1: 95.2 a/o ^{244}Cm

	Concentration			Atom Fraction		
Isotope	Initial, Meas.	Final, Meas.	Final,[a] Calc.	Initial, Meas.	Final, Meas.	Final,[b] Calc.
^{244}Cm	1.000	0.9744	0.974	0.952	0.939	0.939
^{245}Cm	0.00756	0.02326	0.028	0.0072	0.022	0.0203
^{246}Cm	0.04139	0.04129	0.0414	0.0394	0.039	0.0396
Fissions	-	0.0130				

179-2: 94.56 a/o ^{244}Cm

^{244}Cm	1.000	0.9626	0.962	0.9456	0.927	0.927
^{245}Cm	0.01893	0.03531	0.0462	0.0179	0.034	0.036
^{246}Cm	0.03754	0.03843	0.0380	0.0355	0.037	0.036
Fissions	-	~0.0199				

179-3: 56.63 a/o ^{244}Cm

^{244}Cm	1.000	0.9724	0.5663	0.5567	
^{245}Cm	0.007752	0.0234	0.00439	0.0134	
^{246}Cm	0.1035	0.1021	0.0586	0.0585	
^{247}Cm	0.001889	0.002148	0.00107	0.00123	
^{248}Cm	0.6528	0.6468	0.3697	0.3702	
^{249}Bk	0.01106	0.01491			
^{250}Cf	0.000199	0.001734			
^{252}Cf	0.0005192	0.0009325			
Fissions	-	0.01904			

179-4: 50.80 a/o ^{249}Cf

^{249}Cf	1.000	0.9451	0.5080	0.4952
^{250}Cf	0.3623	0.2865	0.1840	0.1501
^{251}Cf	0.1294	0.1892	0.0657	0.0991
^{252}Cf	0.4769	0.4876	0.2423	0.2555
Fissions	-	~0.0597		

Reference Foil

	Initial Conc.	Total Fissions
^{235}U	1.000	0.0228 ±0.002

Cobalt Activity corrected to discharge = 7.74×10^{12} disintegrations/minute-gram.

a. Final calculated concentration of sample defined at time[c] when the calculated ^{244}Cm concentration equaled the measured value.
b. Final calculated atom fraction of sample defined at time[c] when the calculated ^{244}Cm atom fraction equaled the measured value.
c. These times did not agree exactly.

Assembly No. 207 (Bare)

The initial and final concentrations of the curium isotopes in the predominant ^{244}Cm sample are presented in Table II. Calculated results using several methods for determining the total exposure are also presented. This sample had a thermal spectrum and a high exposure as evidenced by a ^{235}U fission burnup of 45%. The first column of calculated results was obtained with the cross section set in Table V for a $(\phi_f/\phi_s) = 2.19$. The exposure was defined as the time where the measured and calculated ^{235}U fission fraction agreed. This method of normalization yields a ^{244}Cm concentration that is too low and a ^{245}Cm concentration that is too high. The next two columns list calculations normalized at the exposure where the measured and calculated ^{244}Cm atom fractions agree. Normalization on the basis of atom fractions was chosen because the ratio of the various curium isotopes can be measured accurately by mass spectrometry, while the determination of absolute concentration has a greater uncertainty. The data included in the next to the last column are improved over that referenced to the ^{235}U fission; however, the predictions of the ^{244}Cm and ^{245}Cm concentrations are not satisfactory.

The last column compares results derived with a reduction in the ^{244}Cm resonance integral. *This adjustment should be thought of in terms of the change in the total effective cross section. A reduction in both the thermal cross section and the resonance integral or a change in the method of formulating an effective cross section from these two components could yield the same effective cross section.* With only this type of change, the results are in excellent agreement with the measured data. By comparison, agreement between calculated and experimental californium concentrations, or the ratio of ^{250}Cf to ^{252}Cf is not as satisfactory. Because the concentrations of the californium isotopes are small and are changing rapidly with exposure, small adjustments in the higher curium isotopes cross sections or in the exposure could improve the agreement with the measured results.

Assembly No. 206 (Lithium-Aluminum)

For the data for ^{6}Li-Al assembly No. 206, (Table III), the same methods of determining total exposure discussed earlier were used. Again the normalization to the ^{235}U fissions does not yield satisfactory agreement. The last two columns with exposure normalized at the measured ^{244}Cm atom fraction again show improved agreement. The last column derived with the reduced ^{244}Cm cross section yields a slightly improved comparison

with the measured results than that derived with no change in the cross sections. The agreement with the ^{250}Cf concentration may be fortuitous because the measured and calculated ^{248}Cm concentrations are not in as good agreement. The ratio of ^{250}Cf to ^{252}Cf is also significantly different, indicating that further adjustments in the ^{250}Cf-^{252}Cf cross sections are probably necessary.

Assembly No. 198

Assembly No. 198 contained samples with ^{244}Cm, ^{246}Cm, and ^{249}Cf as the dominant isotopes. The first sample (198-1) contained relatively large fractions of ^{246}Cm and ^{247}Cm in addition to ^{244}Cm. The computational results with and without the change in the ^{244}Cm cross section gave comparable agreement with the measured data. The ^{246}Cm sample was evaluated where the ^{246}Cm atom fraction equalled the measured value. The agreement for the ^{244}Cm and ^{245}Cm atom fractions is improved when the ^{244}Cm resonance integral is reduced. The ^{247}Cm and ^{248}Cm concentrations, however, do not agree as favorably with the measured results.

The ^{248}Cm results appear to indicate possible experimental error in either the initial or final measured concentrations. Conclusions are difficult to draw from the results of the analyses of this sample because the ^{246}Cm burnup is small ($\sim$2%). Calculating the ^{251}Cf and ^{252}Cf concentrations in the two californium assemblies (198-3,4) was difficult. Adjustments of the $^{250\text{-}251}Cf$ cross sections were attempted in an effort to improve agreement within these two samples with little success. This may indicate an experimental difficulty with one of the assemblies. Although the burnup of these samples (7.9% ^{235}U fissions) was approximately the same as with assembly No. 206, these data did not yield the same consistency with the calculated results.

Assemblies No. 195 and No. 179

The data from assemblies No. 195 and 179 are presented in Tables VII and VIII. Calculated results are presented for specimens 179-1 and 179-2. For the results listed at the exposure where the calculated atom fraction equalled the measured value, reasonable agreement is obtained. This would be expected since the burnup is small and large adjustments in the cross sections would be necessary to make significant changes in the calculated results.

CONCLUSIONS

Irradiation assemblies 206 and 207 provided by far the most reliable data because of the greater burnup and the availability of more precise mass spectrometric data than previously possible.

In general, the data obtained from assemblies 206 and 207 indicate the need for a reduction in the ^{244}Cm cross sections currently used in production calculations (see Appendix B, Table B-1). A similar conclusion was reached after calculating yields for the last high-flux californium charge. When this cross section reduction was made, and the data were normalized to the experimentally-measured atom fraction of ^{244}Cm, the calculated concentrations of each of the curium isotopes (using cross sections in Table B-1 except for the ^{244}Cm modification) were in good agreement with the measured concentration for both the bare and the lithium-aluminum assemblies. Agreement between calculated and measured ^{250}Cf and ^{252}Cf concentrations was somewhat poorer and possibly indicates the need for adjusting the cross sections of these isotopes also.

These data were obtained over a period of several years when there was active interest in the possible development of a reactor for the large-scale production of ^{252}Cf having a spectrum with the majority of the reactions in the resonance region. Since that time, the expected production advantages of a harder neutron spectrum have vanished with increased knowledge of the californium production chain cross sections. Also, demand for ^{252}Cf has not required large production programs. Differential cross section data for some of these isotopes, and theoretically generated differential data for the rest, have eliminated the need for formulation of effective cross sections In the near future, effective cross sections will be derived from a multigroup representation of flux and cross sections. The validity of these formulations of effective cross sections can be evaluated for the experimental data derived in this study and from production data derived in well thermalized charges. The various curium and californium cross sections may then be derived to provide better agreement with data from production and the resonance mockup experiments.

APPENDIX A. Evaluation of the Neutron Energy Spectrum in the Resonance Mockup Assembly

The neutron energy spectrum in the resonance mockup assembly was measured to verify the HAMMER[5] calculated spectrum and to compare with a previously measured spectrum for the resonance reactor. Standard techniques were utilized in which various resonance detectors were simultaneously irradiated in a reference thermal flux and in the resonance mockup assembly. The resonance detectors (^{176}Lu, ^{239}Pu, ^{115}In, ^{197}Au, ^{186}W, and ^{63}Cu) and a ^{235}U reference foil were used in the experiment.

For the thermal reference position, the reaction rate per atom is

$$A_{ref}^{th} = F^{th} \, (g \, \sigma_{2200}) \, \phi^{th} \qquad \text{(A-1)}$$

where,

F = flux depression correction
$(g \, \sigma_{2200})$ = effective thermal cross section
ϕ^{th} = thermal flux

The epicadmium reaction rate per unit atom in the resonance mockup assembly can be divided into a smooth and a resonance component

$$A_{RM}^{epi} = A^{sm} + A^{res} \qquad \text{(A-2)}$$

From known differential cross sections and calculated spectra, the reaction rate due to the resonance only can be derived,

$$A_{RM}^{res} = A_{RM}^{epi} \left(\frac{A^{res}}{A^{sm} + A^{res}} \right) \qquad \text{(A-3)}$$

where,

$$A^{sm} = (F^{sm})(RI)^{sm}(\phi^{sm}) \qquad \text{(A-4)}$$

$$A^{res} = f(F^{res})(RI)^{res}(\phi^{res}) \qquad \text{(A-5)}$$

f = correction for cadmium shielding of resonance

RI = resonance integral

ϕ^{sm} = total epicadmium flux

ϕ^{res} = asymptotic flux per unit lethargy at resonance energy

The ratio of the corrected resonance activity for the gold foil to its thermal reference activity is

$$\frac{(A_{RM}^{res})_{Au}}{(A_{ref}^{th})_{Au}} = \frac{f(F_{Au}^{res})(RI)_{Au}^{res}(\phi_{Au}^{res})}{F_{Au}^{th}\,(g\,\sigma_{2200})_{Au}\,\phi^{th}} \qquad \text{(A-6)}$$

Similarly for isotope x

$$\frac{(A_{RM}^{res})_{x}}{(A_{ref}^{th})_{x}} = \frac{f(F_{x}^{res})(RI)_{x}^{res}(\phi_{x}^{res})}{F_{x}^{th}\,(g\,\sigma_{2200})_{x}(\phi^{th})} \qquad \text{(A-7)}$$

Taking the ratio of equations (A-6) and (A-7) and solving for the ratio of the fluxes at the resonance energies yields

$$\left\{\frac{\phi_{x}^{res}}{\phi_{Au}^{res}}\right\} = \left\{\frac{(A_{RM}^{res})_{x} \,/\, (A_{ref}^{th})_{x}}{(A_{RM}^{res})_{Au} \,/\, (A_{ref}^{th})_{Au}}\right\}\left\{\frac{F_{x}^{th}\,(g\,\sigma_{2200})_{x} \,/\, f(F_{x}^{res})\,(RI)_{x}^{res}}{F_{Au}^{th}\,(g\,\sigma_{2200})_{Au} \,/\, f(F_{Au}^{res})(RI)_{Au}^{res}}\right\} \qquad \text{(A-8)}$$

The derivation of the parameters for substitution into equation (A-8) is straightforward for all of the isotopes except ^{176}Lu and ^{239}Pu, which have subcadmium resonances. For these isotopes, a resonance integral was derived by numerically integrating the subcadmium cross section curve. In addition, the measured activities were corrected for reactions that occurred in the region below the resonance. The resonance integral was evaluated by dividing the cross section curve into regions of equal lethargy interval and then summing up the contributions from each interval (Fig. A-1). For equal lethargy intervals, the resonance integral is equal to the lethargy width times the sum of the average cross section in each interval. A resonance integral can then be evaluated by this technique over any desired total lethargy width.

Figure A-2 illustrates how this technique was applied to the ^{239}Pu resonance. The measured subcadmium activity corresponds to the integral of the reaction rate curve ($\sigma_f\phi$) over the region below the cadmium cutoff. Thus to obtain a flux corresponding to the energy of the resonance, the measured activity is reduced for that activation occurring above and below the area designated as "RI Region." This subcadmium activity was reduced by the ratio of the area in the RI Region to the total area. The resonance integral was evaluated over the RI Region (shown in Figure A-2) by the technique described in Figure A-1. Because the shapes of the cross section curve and the reaction rate curve are similar, the choice of the width of the RI Region was not critical. The same approach was used for the ^{176}Lu resonance.

Standard corrections were made for thermal and resonance self-shielding, nonresonance activation, and resonance overlap by cadmium and ^{235}U in the fuel.[10] The parameters for substitution into equation A-8 and the derived resonance fluxes are listed in Table A-1 and the data, in Figure 7 of the main text. The measured data were normalized so that the flux at the gold resonance coincides with the calculated distribution. The normalized data indicate that the shape of the derived spectrum matches the calculated distribution reasonably well. The slightly higher measured distribution in the subcadmium region was also evidenced by the ^{235}U cadmium ratio, as the measured value of 2.8 indicated a softer spectrum than the calculated value of 2.4.

TABLE A-1. Data for Calculation of Resonance Flux

Isotope	E^{res}, ev	$g\sigma_{2200}$	RI^{res}	RI^{sm}	f	F^{res}/F^{th}	$A^{res}_{RM}/A^{th}_{ref}$	ϕ^{res}
^{235}U	-	561	263	-	-	1.010	2.8[a]	-
^{176}Lu	0.143	3081	-	-	-	0.980	0.188[b]	0.52 ±0.04
^{239}Pu	0.296	777	-	-	-	0.999	0.204[b]	0.57 ±0.06
^{115}In	1.46	156	2487	63	0.937	0.358	0.518	0.80 ±0.05
^{197}Au	4.91	99.4	1490	40	0.985	0.229	0.411	1.00 ±0.03
^{186}W	18.8	35	410[c]	14	-	0.560	0.808	1.08 ±0.22[d]
^{63}Cu	580.	4.5	2.04	1.82	-	0.657	0.119	1.47 ±0.30

a. Cadmium ratio in 0.79 wt % resonance mockup assembly. This ratio includes a 5% correction for shielding of the ^{235}U resonance in the detector foil by the ^{235}U in the fuel tube surrounding the resonance mockup assembly.

b. Subcadmium activity for ^{239}Pu and ^{176}Lu.

c. Includes correction for cadmium shielding of resonance (see reference 10).

d. Includes 5% correction for shielding of ^{186}W resonance by resonances in ^{235}U in fuel tube surrounding the assembly.

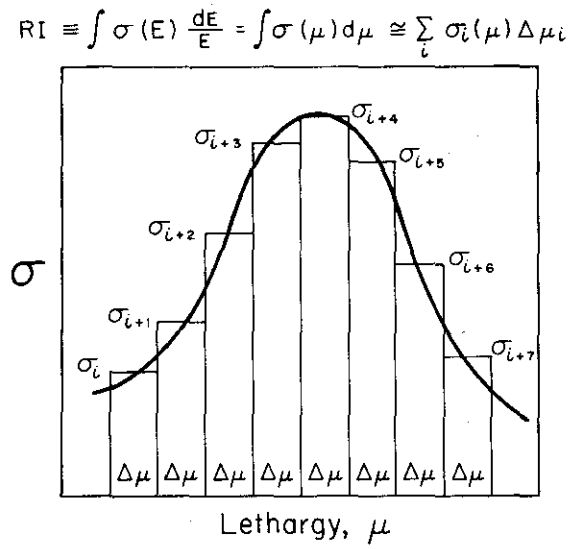

FIGURE A-1. CALCULATION OF RESONANCE INTEGRAL

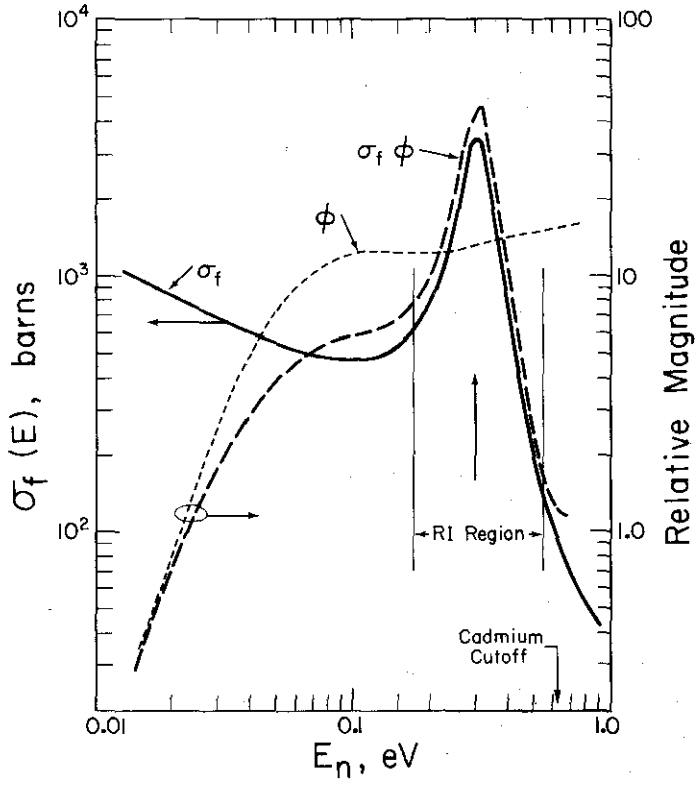

FIGURE A-2. ^{239}Pu RESONANCE ACTIVITY CALCULATION

APPENDIX B. Derivation of Effective Cross Sections

During the past few years, an extensive effort was made at the Savannah River Laboratory (SRL) to improve the precision of the cross sections for the curium and californium isotopes through measurements both on- and off-site. With a portion of the data derived from these measurements and a re-evaluation of some older data, a new consistent set of integral cross sections was derived.[11] This set, which is listed in Table B-1, is assumed to represent the best estimate of cross sections of isotopes in the production chain and was used in the current study.

The evaluation of effective cross sections of the isotopes in the production chain (Figure 1) required the weighting of the thermal cross sections and resonance integrals by factors determined for the fast-to-slow flux ratio of the particular case under consideration.

Since the thermal flux was always taken as the independent variable in solving the isotopic conversion equations, a cross section convention was adopted which was appropriate. Total reaction rates per atom were given by

$$A^{tot} = \phi^{th} \times \overline{\sigma_{tot}} \equiv \phi^{th} \left(\overline{\sigma_{th}} + \overline{\sigma_{epi}}\right) \qquad \text{(B-1)}$$

This convention is consistent, in the thermal group, with the normal result

$$A^{th} = \frac{\int_0^{cutoff} \sigma(E)\ \phi(E)\ dE}{\int_0^{cutoff} \phi(E)\ dE} \qquad \text{(B-2)}$$

This convention yields an epithermal effective cross section that incorporates the fast to thermal absorption ratio with the thermal cross section (Equation B-3).

The thermal portion of the effective cross section was derived for various fast-to-thermal flux ratios from HAMBUR[9] calculations for those isotopes with known differential cross section structure (^{243}Am, ^{244}Cm, ^{245}Cm, and ^{246}Cm). The higher isotopes in the production chain (those with unknown differential structure) were assumed to be 1/v in the thermal region. Figure B-1 illustrates the variation of the effective thermal cross section with flux ratio for the known isotopes and for a 1/v isotope.

TABLE B-1. ^{252}Cf Production Chain Cross Sections

Isotope	σ_{2200}, barns Abs.	Fiss.	Cap/Abs.	Resonance Integral, barns Abs.	Fiss.	Cap/Abs.
^{242}Pu	20	-		1180	-	
^{243}Am	86.6	-		1470	-	
^{244}Cm	3.7	1.1	0.92	663	13	0.98
^{245}Cm	2640	2250	0.15	910	800	0.12
^{246}Cm	1.2	-		121	-	
^{247}Cm	153	98	0.36	1300	800	0.39
^{248}Cm	1.35	-		240	-	
^{249}Bk	1451	-		1240	-	
^{249}Cf	1900	1630		2750	1720	
^{250}Cf	1485	-		4975	-	
^{251}Cf	6910	4930	0.29	2100	1370	0.35
^{252}Cf	28	6		58	12	
^{253}Cf	2250	2235		2250	2235	
^{254}Cf	100	-		100	-	

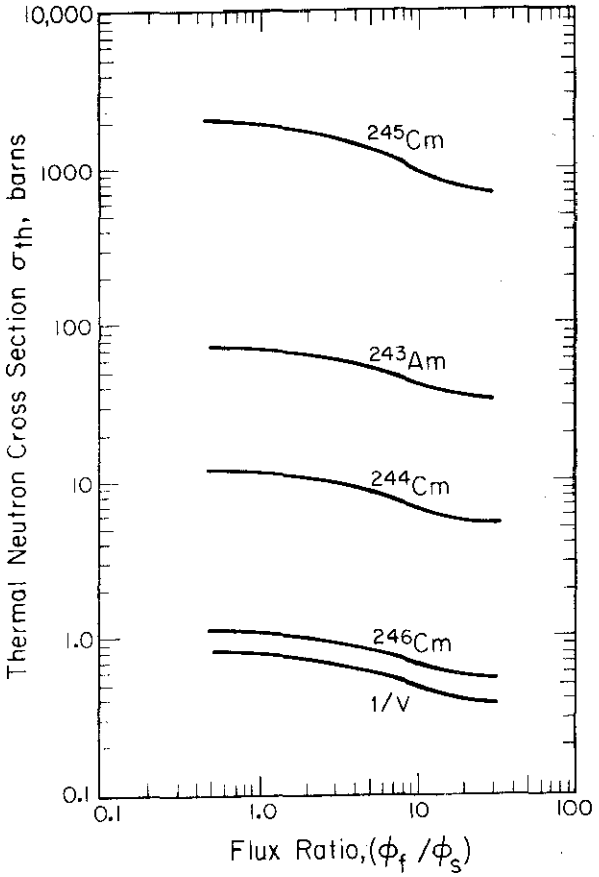

FIGURE B-1. VARIATION OF EFFECTIVE THERMAL NEUTRON CROSS SECTIONS WITH (ϕ_f/ϕ_s)

The fast portion of the effective cross section was derived from a correlation between infinitely dilute resonance integrals, RI^{∞}, and effective fast cross sections for isotopes of known differential structure. The effective fast (epithermal) cross section, $\overline{\sigma_{epi}}$, was defined in terms of the effective thermal cross section from HAMBUR, $\overline{\sigma_{th}}$, and the HAMBUR neutron balance of fast-to-slow absorptions,

$$\overline{\sigma_{epi}} = \overline{\sigma_{th}} \times \left(\frac{\text{fast absorptions}}{\text{slow absorptions}} \right) \qquad \text{(B-3)}$$

Figure B-2 illustrates the relationship between RI^{∞} and $\overline{\sigma_{epi}}$ for a fast-to-slow flux ratio of 3.5. Results for even-odd and odd-odd nuclei are included on the same graph, and a smooth curve has been drawn through the data points. Although a different correlation is theoretically expected for the two different types of nuclei, the small variation in the data doesn't warrant a separate fit. For those isotopes above ^{246}Cm in the production chain where only the resonance integral is known, $\overline{\sigma_{epi}}$ can be derived from this curve. Similar correlations were made for other fast-to-slow flux ratios, and values of $\overline{\sigma_{epi}}$ obtained from those correlations were plotted for each isotope as a function of (ϕ_f/ϕ_s). Results for the nuclei of interest are presented in Figure B-3.

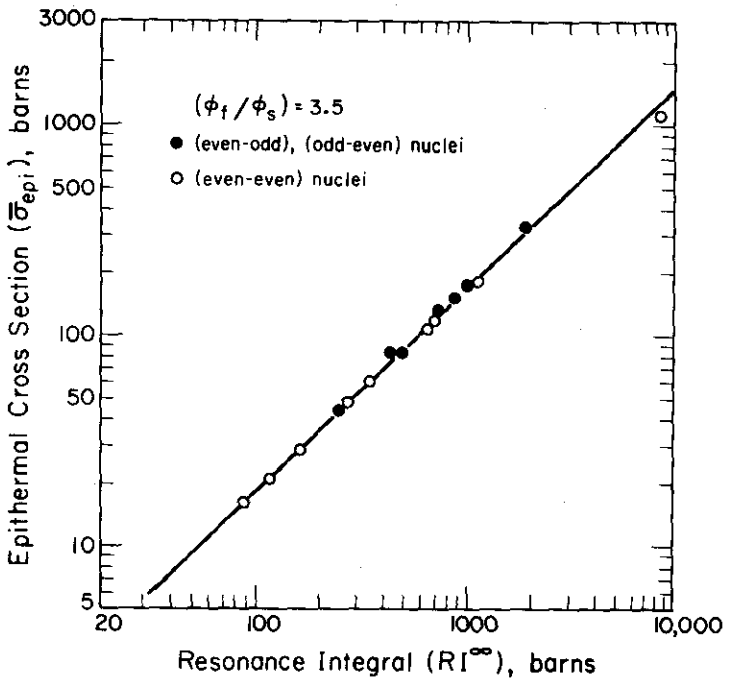

FIGURE B-2. EPITHERMAL CROSS SECTION vs RESONANCE INTEGRAL FOR ISOTOPES OF KNOWN STRUCTURE

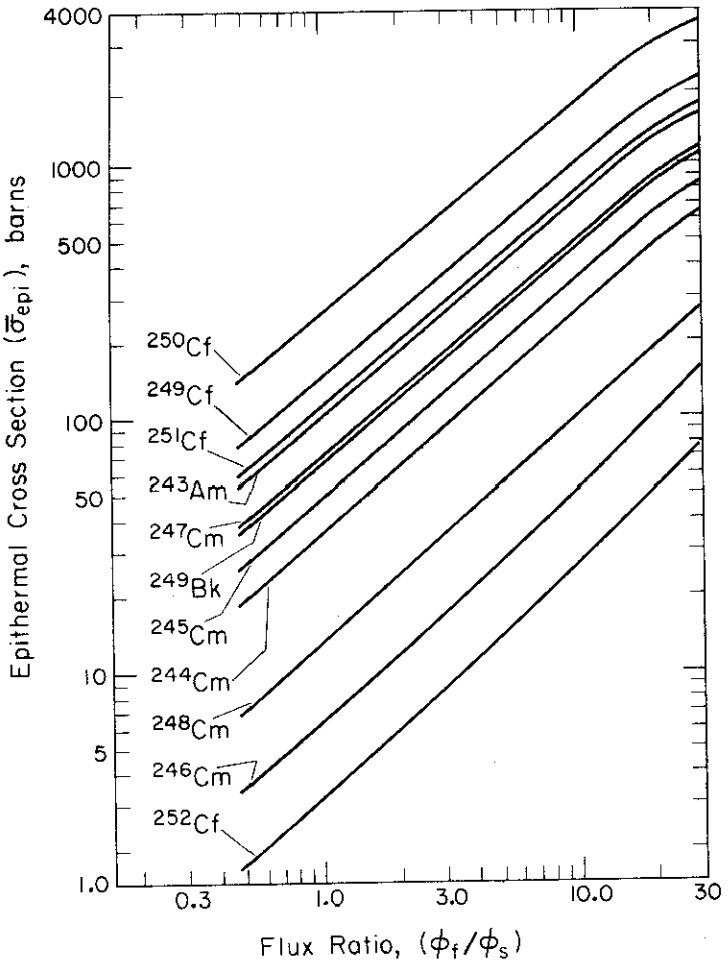

FIGURE B-3. VARIATION OF EFFECTIVE EPITHERMAL CROSS SECTIONS WITH FLUX RATIOS

The effective thermal and fast cross sections were combined to yield a total effective value

$$\overline{\sigma_{total}} = \overline{\sigma_{th}} + \overline{\sigma_{epi}} \qquad \text{(B-4)}$$

Figure B-4 illustrates the variation of $\overline{\sigma}_{total}$ with the fast-to-slow flux ratio. In the evaluation of a reaction rate, this quantity should be multiplied by the thermal flux in the target. The cross sections listed in Table V of the main text were derived from Figures B-1 and B-3 for the specified fast-to-slow flux ratios, $(\phi_f/\phi s)$. For the irradiation assemblies other than No. 206 and No. 207, the cross sections were derived from these figures for the flux ratios listed in Table IV.

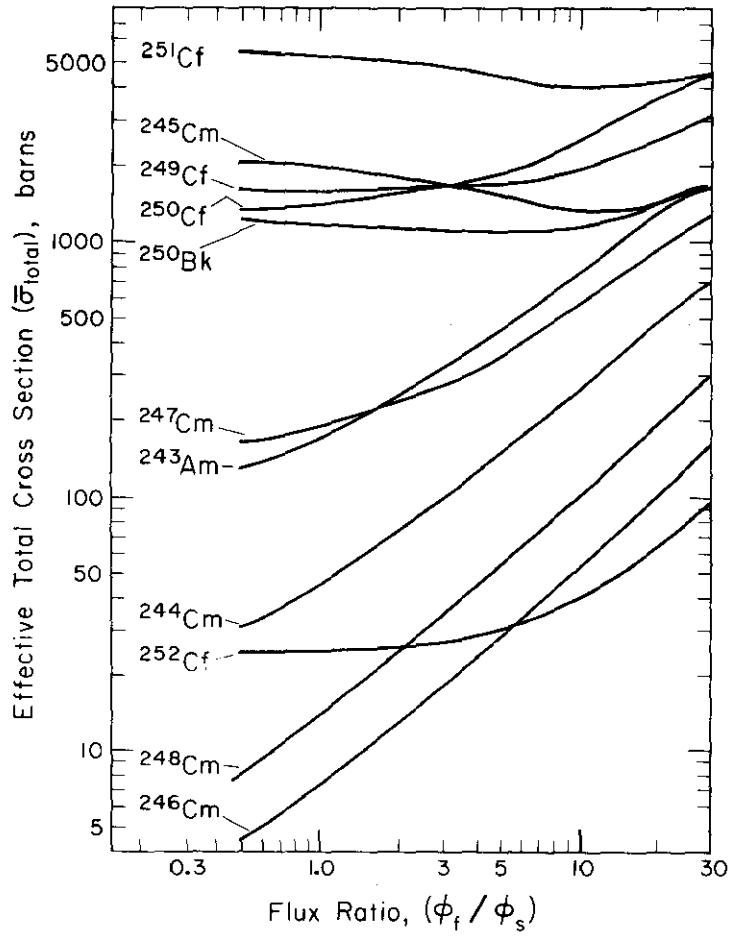

FIGURE B-4. VARIATION OF EFFECTIVE TOTAL CROSS SECTIONS WITH FLUX RATIOS

REFERENCES

1. J. L. Crandall, compiler. *The Savannah River High Flux Demonstration.* USAEC Report DP-999. E. I. du Pont de Nemours and Co., Savannah River Laboratory, Aiken, South Carolina 29801 (June, 1965).

2. A. Prince. "Nuclear and Physical Properties of Cf-252." *Californium-252.* Proc. Symposium, New York Metropolitan Section of the Amer. Nucl. Soc., New York City, Oct. 22, 1968. USAEC Report CONF-681032, pp. 23-130 (January 1969).

3. C. E. Jewell, S. C. Burnett, D. J. Pellarin, and R. M. Satterfield. *Displaced Moderator Resonance Reactor Experiments.* USAEC Report DP-1281. E. I. du Pont de Nemours and Co., Savannah River Laboratory, Aiken, South Carolina 29801 (November, 1971).

4. J. D. Spencer and N. P. Baumann. "A Resonance Spectrum Irradiation Assembly for Evaluation of ^{252}Cf Production Cross Sections." *Trans. Amer. Nucl. Soc.* 14, 380-381 (1971).

5. J. E. Suich and H. C. Honeck. *The HAMMER System.* USAEC Report DP-1064. E. I. du Pont de Nemours and Co., Savannah River Laboratory, Aiken, South Carolina 29801 (January, 1967).

6. F. L. Lisman, R. M. Abernathey, W. J. Maeck and J. E. Rein. "Fission Yields of Over 40 Stable and Long-Lived Fission Products for Thermal Neutron Fissions ^{233}U, ^{235}U, ^{239}Pu, and ^{241}Pu and Fast Reactor Fissioned ^{235}U and ^{239}Pu." *Nucl. Sci. and Eng.*, 42, 191 (1970).

7. R. M. Harbour and K. W. MacMurdo. "Mass Yields from Thermal-Neutron Induced Fission of ^{245}Cm." *J. Inor. Nucl. Chem.* 34, 2109 (1972).

8. H. F. Aly and R. M. Latimer. "Variables Affecting Ion-Exchange for Inter-Actinide Separations." *J. of Inorg. and Nucl. Chem.* 29, 2041 (1967).

9. D. R. Finch and R. P. Christman. *The HAMBUR System.* USAEC Report DP-1283. E. I. du Pont de Nemours and Co., Savannah River Laboratory, Aiken, South Carolina 29801 (February, 1972).

10. N. P. Baumann. *Resonance Integrals and Self-Shielding Factors for Detector Foils.* USAEC Report DP-817. E. I. du Pont de Nemours and Co., Savannah River Laboratory, Aiken, South Carolina 29801 (January, 1963).

11. E. J. Hennelly. "The Heavy Actinide Cross Section Story." *Proceedings of the Third Conference on Neutron Cross Sections and Technology, March 1971, Knoxville.* CONF-710301, Vol. 2, p. 714. USAEC-TIC, Oak Ridge, Tennessee (1971).